NASA/TM—2018-219939

Modeling of Time-Dependent Strength Degradation of SiC/SiC Ceramic Matrix Composites via MAC/GMC Computer Code

Subodh K. Mital
The University of Toledo, Toledo, Ohio

Steven M. Arnold, Pappu L.N. Murthy, Brett A. Bednarcyk, and Evan J. Pineda
Glenn Research Center, Cleveland, Ohio

August 2018

NASA STI Program . . . in Profile

Since its founding, NASA has been dedicated to the advancement of aeronautics and space science. The NASA Scientific and Technical Information (STI) Program plays a key part in helping NASA maintain this important role.

The NASA STI Program operates under the auspices of the Agency Chief Information Officer. It collects, organizes, provides for archiving, and disseminates NASA's STI. The NASA STI Program provides access to the NASA Technical Report Server—Registered (NTRS Reg) and NASA Technical Report Server—Public (NTRS) thus providing one of the largest collections of aeronautical and space science STI in the world. Results are published in both non-NASA channels and by NASA in the NASA STI Report Series, which includes the following report types:

- TECHNICAL PUBLICATION. Reports of completed research or a major significant phase of research that present the results of NASA programs and include extensive data or theoretical analysis. Includes compilations of significant scientific and technical data and information deemed to be of continuing reference value. NASA counter-part of peer-reviewed formal professional papers, but has less stringent limitations on manuscript length and extent of graphic presentations.

- TECHNICAL MEMORANDUM. Scientific and technical findings that are preliminary or of specialized interest, e.g., "quick-release" reports, working papers, and bibliographies that contain minimal annotation. Does not contain extensive analysis.

- CONTRACTOR REPORT. Scientific and technical findings by NASA-sponsored contractors and grantees.

- CONFERENCE PUBLICATION. Collected papers from scientific and technical conferences, symposia, seminars, or other meetings sponsored or co-sponsored by NASA.

- SPECIAL PUBLICATION. Scientific, technical, or historical information from NASA programs, projects, and missions, often concerned with subjects having substantial public interest.

- TECHNICAL TRANSLATION. English-language translations of foreign scientific and technical material pertinent to NASA's mission.

For more information about the NASA STI program, see the following:

- Access the NASA STI program home page at http://www.sti.nasa.gov

- E-mail your question to help@sti.nasa.gov

- Fax your question to the NASA STI Information Desk at 757-864-6500

- Telephone the NASA STI Information Desk at 757-864-9658

- Write to:
  NASA STI Program
  Mail Stop 148
  NASA Langley Research Center
  Hampton, VA 23681-2199

NASA/TM—2018-219939

Modeling of Time-Dependent Strength Degradation of SiC/SiC Ceramic Matrix Composites via MAC/GMC Computer Code

Subodh K. Mital
The University of Toledo, Toledo, Ohio

Steven M. Arnold, Pappu L.N. Murthy, Brett A. Bednarcyk, and Evan J. Pineda
Glenn Research Center, Cleveland, Ohio

National Aeronautics and
Space Administration

Glenn Research Center
Cleveland, Ohio 44135

August 2018

This work was sponsored by the
Transformative Aeronautics Concepts Program.

Level of Review: This material has been technically reviewed by technical management.

Available from

NASA STI Program
Mail Stop 148
NASA Langley Research Center
Hampton, VA 23681-2199

National Technical Information Service
5285 Port Royal Road
Springfield, VA 22161
703-605-6000

This report is available in electronic form at http://www.sti.nasa.gov/ and http://ntrs.nasa.gov/

Modeling of Time-Dependent Strength Degradation of SiC/SiC Ceramic Matrix Composites via MAC/GMC Computer Code

Subodh K. Mital
The University of Toledo
Toledo, Ohio 43606

Steven M. Arnold, Pappu L.N. Murthy, Brett A. Bednarcyk, and Evan J. Pineda
National Aeronautics and Space Administration
Glenn Research Center
Cleveland, Ohio 44135

Abstract

Silicon carbide fiber reinforced silicon carbide (SiC/SiC) ceramic matrix composites (CMCs) display time-dependent strength degradation at intermediate temperatures (600 to 900 °C). This is generally believed to be an oxidation induced phenomenon. The understanding of the effect of temperature with environment (oxidation) is key towards development of SiC/SiC CMCs with a reliable load carrying capacity. Various theories have been proposed to explain the strength degradation. One suggests that the boron nitride (BN) coating deposited on the fibers oxidizes causing fusion of fibers. Another theory proposes that the SiC fibers are oxidized forming a silica scale leading to premature fiber failure. A more recent theory suggests that SiC fiber strength is intrinsically time-dependent due to slow crack growth of flaws in the fibers. An empirical model, termed as "fiber classic model", which is based on a standard slow crack growth type power-law, has been implemented within NASA's micromechanics-based MAC/GMC computer code as a user routine. Model parameters for this "classic model" were calibrated from stress-rupture data of Hi-Nicalon™ monofilaments using the maximum likelihood estimation (MLE) technique. This new capability in the MAC/GMC computer code was then used to predict the stress-rupture behavior of Hi-Nicalon™ tows as well as 2-D SiC/SiC composites reinforced with Hi-Nicalon™ fibers. Results demonstrate that the MAC/GMC with this new capability successfully predicts the time-to-failure versus applied stress within the intermediate temperature range at various scales as well as laminated composites in an oxidizing environment.

Introduction

Ceramic matrix composites are increasingly being used in gas turbine engines for their superior high-temperature properties and potential weight savings when compared to traditional metallic materials. SiC/SiC composites are particularly attractive, with both continuous fiber laminates and woven reinforcements finding significant engine applications (Ref. 1). However, a major issue with SiC/SiC composites is their susceptibility to strength degradation at intermediate temperatures (600 to 900 °C) in an oxidizing environment when subjected to constant stresses above the proportional limit stress (PLS) (Ref. 2). The PLS, sometimes referred to as first matrix cracking stress, is an important design parameter for CMCs and is associated with the onset of nonlinearity in the stress-strain response of the composite. This strength degradation phenomenon is believed to be an environmental (oxidation-induced) phenomenon (Ref. 3). The phenomenon has also been referred to in the literature as delayed-failure, static fatigue, and stress-rupture. Clearly, the understanding of the effects of temperature and environment on fiber strength is very important for the development of durable SiC/SiC composites with reliable load carrying capacity. It should also be noted that creep is not observed in these composites below 1000 °C (Ref. 3).

Many researchers have studied the phenomenon of time-dependent strength degradation of SiC fibers. Various mechanisms have been proposed in the literature to explain this phenomenon. Sullivan (Ref. 4) has summarized these findings and categorized the theories into three groups. All of these theories agree that the root mechanism associated is an oxidation-reaction that occurs at the intermediate temperature range (600 to 900 °C).

The first group of researchers (Refs. 5 to 8) attribute the loss of strength over time to "embrittlement" of the composite. This is due to the reaction of the oxidizing environment with the fiber-matrix interphase material, which consists of a boron nitride (BN) coating on the fiber. According to this mechanism, the presence of oxygen causes the BN coating to oxidize resulting in fusion of fibers to one another and to the matrix, resulting in a brittle composite. This fusion promotes local load sharing in that if one fiber fails, it then overloads the neighboring (fused) fibers making it more likely for them to fail. This then results in a cascade of failures, causing the composite to fail with time at a stress that is much lower than the static (fast fracture) strength. This mechanism is consistent with delayed failure or reduced strength over time since oxidation of the interphase material (BN) is a time-dependent phenomenon and it increases with time. Thus the "embrittlement", or the fusion of the fibers, also increases with time, resulting in lower strength values as time progresses.

The second group of researchers (Refs. 9 and 10) suggest that the presence of oxygen causes the silicon carbide fibers themselves to oxidize and form a silica (SiO_2) scale. Because of the difference in volume of the silica scale and silicon carbide, a tensile stress is induced in the fibers, causing a "premature" fiber failure. The thickness of the silica scale increases with time, thus the theory appears to be consistent with time-dependent strength degradation. These researchers also claim that the matrix and fibers in the vicinity of a matrix crack also oxidize, tending to force open the crack. This causes a spike in the tensile stresses in the fibers bridging the crack. Both of these proposed mechanisms would cause tensile stress in the fiber to increase with time as the amount of oxide grows, thus resulting in strength degradation with time.

The third group of researchers, most notably Lamon from University of Bordeaux, France (Refs. 3, 11, and 12), suggest that the time-dependent failure of silicon carbide fibers is because of slow crack growth of inherent flaws in the fibers. This theory is based on experimental data, fractography, and modeling. The process is activated by oxidation and flaw sizes increase with oxidation and thus with time resulting in strength degradation. These researchers also suggest that the time-dependent failure is caused by slow crack growth of surface defects by oxidation of grain boundaries (free carbon) and SiC grains at the crack tip. A recent report by Sullivan (Ref. 4) following this third theory has formulated a three-way relationship between time, stress, and probability of failure. A similar approach has been used to develop empirical models, which have been successfully applied to assess Kevlar and carbon fiber reinforced composite overwrapped pressure vessels (COPV) failures under sustained loads (Ref. 13).

Following the fiber slow crack growth mechanism proposed in References 3, 11, 12, the objective of this paper is to assess the applicability of an empirical slow crack growth model to explain the time-dependent strength degradation in SiC fibers and SiC/SiC composites. This model has been implemented in NASA's multiscale micromechanics-based code MAC/GMC (Ref. 14) as a user routine and then used to predict the composite response. It should be noted that no other mechanisms such as the oxidation of fiber coating or the oxidation of the fiber itself, are considered in the present study.

MAC/GMC Computer Code

MAC/GMC is NASA's micromechanics-based computer code for multiscale composite analysis (Ref. 14). Macroscale analyses, which treat the composite as a homogeneous, anisotropic material, can be more efficient compared to micromechanics, particularly when combined with large scale structural analyses. However, utilizing micromechanics to analyze the composite behavior has its own advantages. Micromechanics enables one to account explicitly for variations in constituent material properties as well as microstructural effects, such as fiber volume content, fiber packing and orientation, making it a robust

analysis tool for prediction of failure in composites. Moreover, interactive effects between the constituents in the composites are accounted for automatically, rather than through the postulation of an anisotropic continuum damage model.

At the core of the MAC/GMC software are the Generalized Method of Cells (GMC), first developed by Paley and Aboudi (Ref. 15) and the High-Fidelity Generalized Method of Cells (HFGMC), first developed by Aboudi et al. (Ref. 16), are semi-analytical in nature, and their formulation involves application of governing equations in an average sense. They provide the local constituent fields in composite materials, allowing incorporation of arbitrary inelastic constitutive models with various deformation and damage constitutive laws. Herein, the GMC micromechanics model has been employed.

The microstructure of a periodic material, within the context of GMC is represented by a rectangular (doubly-periodic) or parallelepiped (triply-periodic) repeating unit cell (RUC) consisting of an arbitrary number of subcells, each of which may be a distinct material (Fig. 1). In the case of GMC the displacement field is assumed linear,

$$u_i^{(\alpha\beta\gamma)} = w_i^{(\alpha\beta\gamma)} + \bar{y}_1^{(\alpha)} \chi_i^{(\alpha\beta\gamma)} + \bar{y}_2^{(\beta)} \phi_i^{(\alpha\beta\gamma)} + \bar{y}_3^{(\gamma)} \psi_i^{(\alpha\beta\gamma)} \tag{1}$$

where $(\alpha\beta\gamma)$ denotes the subcell number (see Figure 1(b)), $u_i^{(\alpha\beta\gamma)}$ are the components of the subcell displacement field, $w_i^{(\alpha\beta\gamma)}$ are the displacement components at the subcell centroid, $\bar{y}_i^{(\bullet)}$ are Cartesian coordinates at the centroid of each subcell, and $\chi_i^{(\alpha\beta\gamma)}$, $\phi_i^{(\alpha\beta\gamma)}$, and $\psi_i^{(\alpha\beta\gamma)}$ are unknown microvariable that define the displacement field. This linear displacement field leads to a piecewise constant strain field. Displacement and traction continuity is enforced in an average, or integral sense at each of the subcell interfaces and the periodic boundaries of the RUC. These continuity conditions are used to formulate a strain concentration matrix, per subcell, $\mathbf{A}^{(\alpha\beta\gamma)}$, which gives all the local subcell strains, $\boldsymbol{\epsilon}^{(\alpha\beta\gamma)}$ in terms of the global, average, applied strains, $\bar{\epsilon}$

$$\boldsymbol{\varepsilon}^{(\alpha\beta\gamma)} = \mathbf{A}^{(\alpha\beta\gamma)} \, \bar{\boldsymbol{\varepsilon}} \tag{2}$$

The local subcell stresses, $\boldsymbol{\sigma}^{(\alpha\beta\gamma)}$ can then be calculated using the local constitutive law as

$$\boldsymbol{\sigma}^{(\alpha\beta\gamma)} = \mathbf{C}^{(\alpha\beta\gamma)} \mathbf{A}^{(\alpha\beta\gamma)} \, \bar{\boldsymbol{\varepsilon}} \tag{3}$$

Where $\mathbf{C}^{(\alpha\beta\gamma)}$ is the stiffness matrix of the material occupying subcell $(\alpha\beta\gamma)$. The global, average stresses are obtained from a volume-weighted sum of the local subcell stresses, providing the global, effective elastic constitutive equation for the composite,

$$\bar{\boldsymbol{\sigma}} = \mathbf{C}^* \, \bar{\boldsymbol{\varepsilon}} \tag{4}$$

with the effective stiffness matrix given by,

$$\mathbf{C}^* = \frac{1}{DHL} \sum_{\alpha=1}^{N_\alpha} \sum_{\beta=1}^{N_\beta} \sum_{\gamma=1}^{N_\gamma} d_\alpha h_\beta l_\gamma \, \mathbf{C}^{(\alpha\beta\gamma)} \mathbf{A}^{(\alpha\beta\gamma)} \tag{5}$$

where d_α, h_β, and l_γ are the subcell dimensions, and the remaining variables are defined in Figure 1(b). The detailed derivation of GMC including material inelasticity and thermal strains, as well as how the model is embedded within classical laminate theory, are described thoroughly in Aboudi et al. (Ref. 16).

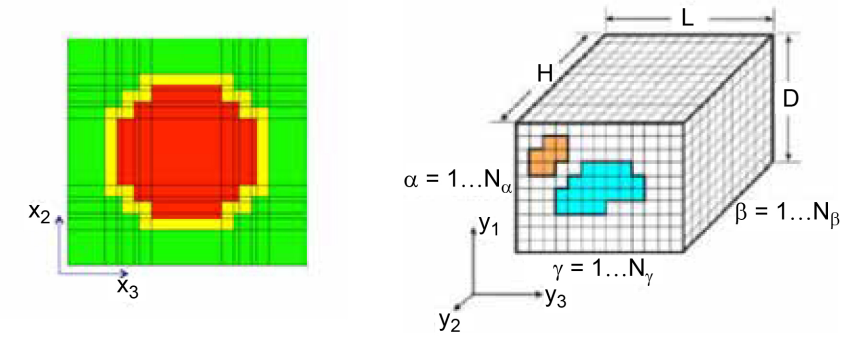

Figure 1.—Composite with repeating microstructure and arbitrary constituents. (a) Doubly-periodic. (b) Triply Periodic.

The semi-analytical formulation of GMC and its implementation into MAC/GMC offer significant computational efficiency to obtain the response (e.g., effective properties, global and local (constituent) stress and strain fields) of a volume element of a material. Further, GMC is ideal for implementation within a multiscale framework; wherein the higher (structural) scale is modeled using the finite element method (FEM) and the material point response is modeled using GMC. FEAMAC is a synergistic multiscale framework, also developed by NASA Glenn, which couples the micromechanics directly to the FEM and is capable of modeling advanced composite structures.

Fiber Classic Model

It is customary in modeling brittle materials to utilize a Weibull statistics based approach to fit stress-rupture life data. Stress rupture is a failure mode of a structure under sustained load and time. It is understood mainly on a phenomenological level and stress rupture life prediction methodologies are generally based on stochastic modeling. Following observations/assumptions are made regarding stress rupture life modeling—(a) stress rupture lifetime is mainly a function of fiber stress, (b) stress rupture is a material property of the fiber i.e., different fibers have different stress rupture characteristics, (c) stress rupture life data can be fit using a two-parameter Weibull distribution. There are a number of models that exist with some variations and generally all are empirical in nature because actual failure mechanism is not really known. Davidge et al. (Ref. 17) developed an equation relating the probability of failure, applied stress and time-to-failure for ceramic materials. Their equation has a similar form as a standard slow crack growth equation and assumed that the crack growth velocity is proportion to the stress intensity factor. Herein, the so called "Classic Model" for stress rupture initially pioneered by Coleman (Ref. 18) and further developed by other researchers has been used. According to the fiber classic model, the relationship between stress-time-temperature is as follows:

$$F(t:\sigma) = 1 - exp\left[-\left\{\int_0^t \left(\frac{\sigma(t)}{\sigma_{ref}}\right)^{\rho} \left(\frac{1}{t_{ref}}\right) dt\right\}^{\beta}\right] \tag{6}$$

Where F is the probability of failure of a fiber in time t due to an arbitrarily varying stress $\sigma(t)$, and σ_{ref} is the Weibull scale parameter for fast fracture strength and t_{ref}, ρ, β are model parameters. As mentioned before, this empirical model is based on a Weibull distribution framework for strength and time, and as mentioned before σ_{ref} can be approximated as the Weibull scale parameter for fast-fracture strength. The quantity (σ/σ_{ref}) is sometimes referred to as stress-ratio. If the applied stress is constant during the time interval t, then the Equation (6) above reduces to a simpler form as:

$$F(t|\sigma) = 1 - exp\left[-\left\{\left(\frac{\sigma}{\sigma_{ref}}\right)^{\rho}\left(\frac{t}{t_{ref}}\right)\right\}^{\beta}\right] \quad (7)$$

Model parameters t_{ref}, ρ, β are usually estimated from test data using the maximum likelihood estimation (MLE) technique. The model implies that different fibers have different lifetimes due to the same applied load. The reason is that different fibers have different initial strength or flaws of different initial sizes.

Based on this model, a series of reliability quantile curves can be developed for use in design that allow estimation of the lifetime for a chosen quantile. Or in other words, this approach can be used by choosing an appropriate combination of stress ratio and lifetime to ensure a desired reliability. These types of curves, referred to as simply design curves or reliability quantile curves, are widely used.

Progressive Failure

To simulate, the time-dependent strength degradation of SiC fibers, a time-marching algorithm has been implemented in NASA's MAC/GMC computer code as a user-routine. This algorithm assigns a random initial probability of failure, P_f (essentially an initial strength) to each fiber by drawing from a uniform random number between [0, 1]. For a given time-step, the code computes the stress in each fiber due to the applied load and this is assumed to be constant for a given time-step. A probability of failure for each fiber is then computed using Equations (6) and (7) above, and the fiber is assumed to have failed if the following condition is satisfied $(P_f)_{computed} \geq (P_f)_{initial}$. The stiffness of the failed fibers is immediately reduced to near zero, and the stresses that were carried by the failed fibers are redistributed to nonfailed fibers. The analysis marches on to the next time step and the process is repeated until all fibers or the composite material fails.

It should be noted that as fibers fail, the stress on fibers that have not failed increases. Thus there is a history dependence of the fiber stress that needs to be taken into account for proper computation of the probability of failure. Thus Equation (7) is appropriately modified as follows:

$$F(t|\sigma) = 1 - exp\left[-\left\{\left(\frac{t_1}{t_{ref}}\right)\left(\frac{\sigma_1}{\sigma_{ref}}\right)^{\rho} + \sum_{i=1}^{i=n}\left(\frac{t_{i+1}-t_i}{t_{ref}}\right)\left(\frac{\sigma_{i+1}}{\sigma_{ref}}\right)^{\rho}\right\}^{\beta}\right] \quad (8)$$

Equation (8) algorithm has been implemented in the MAC/GMC computer code. Stress on a single filament with time is shown in Figure 2 schematically. This approach is very similar to accumulating damage in Miner's rule for fatigue. The stress in a filament for the first time step t_1 is σ_1, for second time step t_2 is σ_2 etc. In general, for the time step t_i, the filament is subjected to a constant stress σ_i during that time step. This "Classic Model" and its variations have been successfully utilized for assessing Kevlar and Carbon fiber reinforced composite overwrapped pressure vessels (COPV) under sustained loads (Ref. 13).

A flow-chart of the progressive failure used for dry tows or composites is shown in Figure 3.

Material System

The material system evaluated in this study is a Hi-Nicalon fiber-reinforced melt-infiltrated (MI) silicon carbide composite. The fibers are woven in a five-harness satin weave. The overall fiber volume fraction is approximately 34 percent and each fiber tow of Hi-Nicalon contains 500 monofilaments of average diameter of 14 μm. The filaments also have a thin (0.5 μm) interphase coating of boron nitride (BN) material. The composite has a small amount of porosity (4 to 5 percent by volume). The proportional limit stress (PLS) of this material is approximately 125 MPa at these intermediate (500 to 800 °C) temperatures (2). The constituent properties of this composite are shown in Table I.

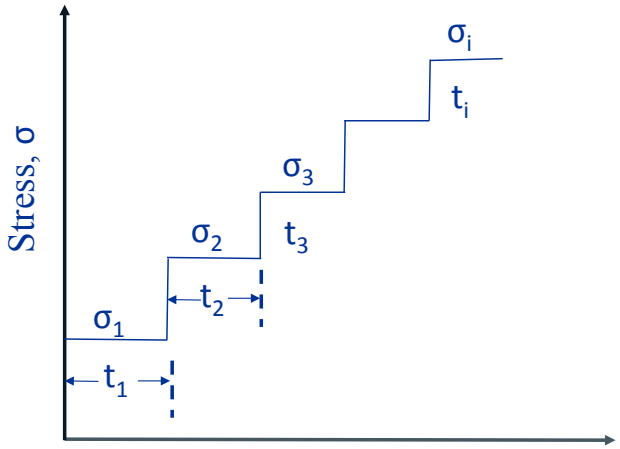

Figure 2.—Stress history with time.

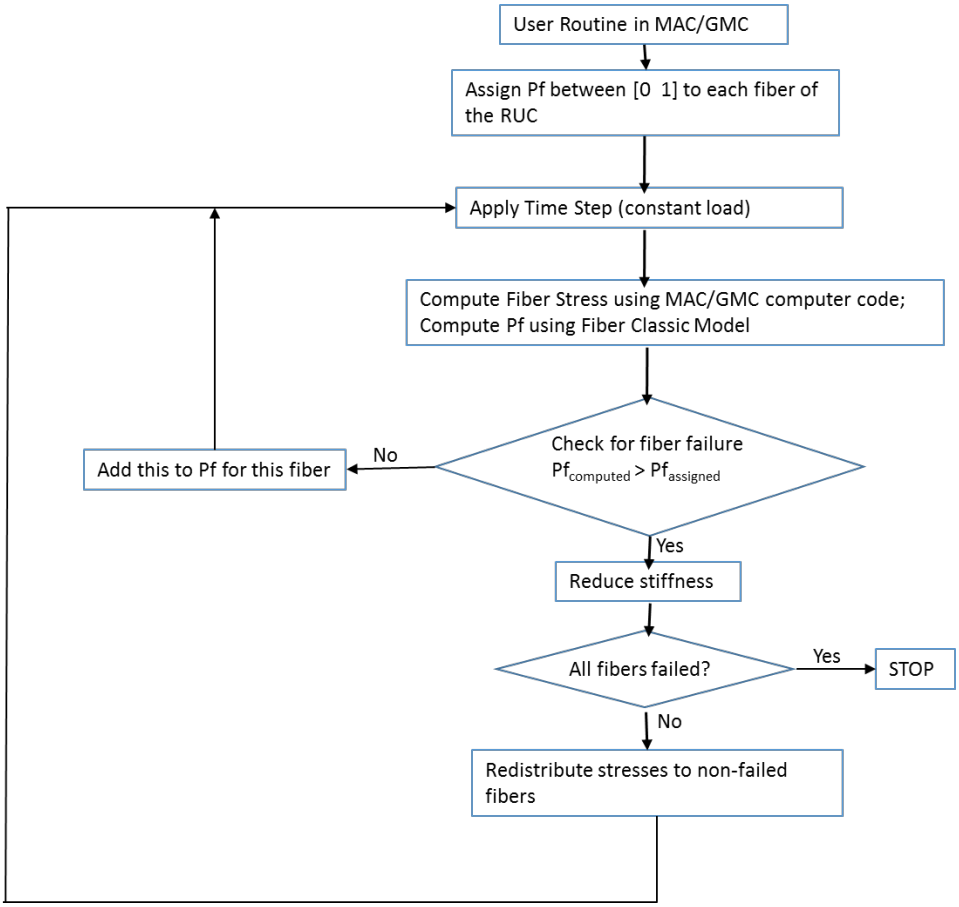

Figure 3.—Flow chart of the progressive failure user-routine in MAC/GMC computer code.

TABLE I.—COMPOSITE CONSTITUENT PROPERTIES AT 800 °C

Constituent	Material	Elastic modulus, GPa	Poisson's ratio	Strength, MPa
Fiber	Hi-Nicalon	280	0.3	[a]2540
Interphase	Boron Nitride	7.0	0.17	70
Matrix	MI-SiC	330	0.17	240

[a]Weibull scale parameter

Results/Discussions

Gauthier and Lamon (Ref. 3) have performed numerous tests on Hi-Nicalon single filaments as well as Hi-Nicalon tows at 800 °C under various applied stresses. Results, shown in Figure 4, show that Hi-Nicalon fibers display strength degradation over time. Although the data displays significant scatter, the rupture times seem to decrease when the applied stresses are increased. However, the trend with the tows is not as clear. According to Gauthier and Lamon (Ref. 3), this behavior is very similar to bulk ceramics, which results from the presence of flaws of different initial sizes. Morscher et al. (Ref. 7) have tested and published data for a Hi-Nicalon fiber reinforced, melt-infiltrated SiC/SiC composite. The tests were performed at temperatures of 815 and 880 °C. These data also show a time-dependent strength degradation. Morscher et al. (Ref. 7) also imply that if the applied stresses were below the proportional limit stress (PLS) which in this composite is approximately 125 MPa, then there is a run-out i.e., the rupture times appear to be > 1.0 million seconds. The single filament data shown in Figure 4 were fitted to the model described above via Equations (6) to (8) using the maximum likelihood estimation (MLE) technique (Ref. 19). The best fit parameters for the fiber classic model found using the maximum likelihood estimation technique are shown in Table II.

Single filament stress-rupture is simulated using these parameters and the results are shown in Figure 5. The simulation data show a standard power-law type of behavior, as expected, at various values of probability of failure (P_f). The simulations clearly capture a three-way relationship among time, stress, and probability of failure. These curves can also be seen as design curves, in the sense that given lifetime desired at a given reliability (probability of failure), the curve indicates the maximum stress that can be applied on a single filament.

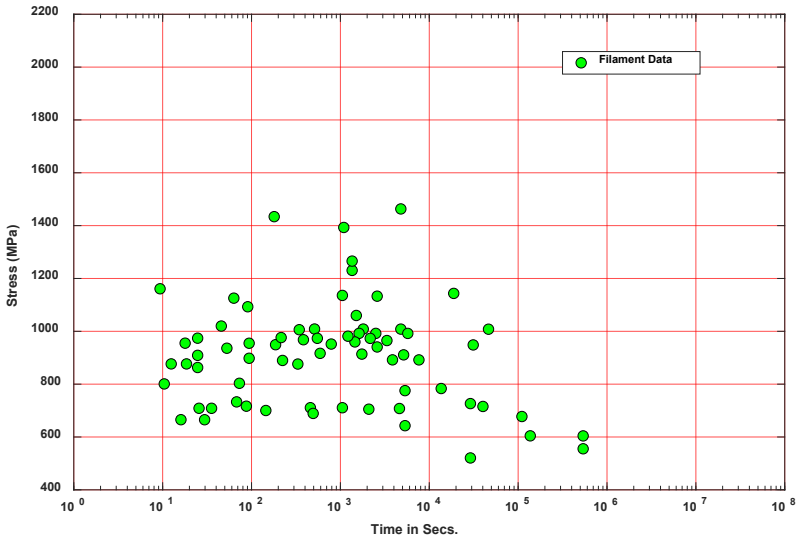

Figure 4.—Stress versus Time-to-failure for single Hi-Nicalon filaments at 800 °C from Reference 9.

TABLE II.—PARAMETERS FOR SINGLE HI-NICALON FIBERS AT INTERMEDIATE TEMPERATURES

t_{ref}, s	σ_{ref}, MPa	ρ	β
26.9	2540	4.44	0.428

Stress versus time-to-failure was also predicted for dry Hi-Nicalon fiber tows using the parameters calibrated for single filaments shown in Table II. Each tow consists of 500 single filaments. The GMC model employed within the MAC/GMC computer code assumes a global load sharing, i.e., the load that was carried by a failed filament is redistributed equally to all nonfailed fibers. Once a single fiber fails, its stiffness is reduced to near zero. Thus, it is assumed that there is no local load sharing, no touching fibers, nor twisting of the tows. For each applied stress level, 100 simulations were run and the results from those simulation are shown in Figure 6. Simulations show a qualitative trend similar to that for single filaments, i.e., the time to failure decreases as the applied stress on the tow is increased. The measured data shows slightly more scatter and irregular behavior. Simulations show that the predicted scatter in the time to failure is much less than what was observed for the single filaments/fibers. As mentioned before, since the simulations do not account for local load sharing, fiber touching or twisting of the tows may lead to a prediction of reduced scatter in the time to failure versus stress in the tows.

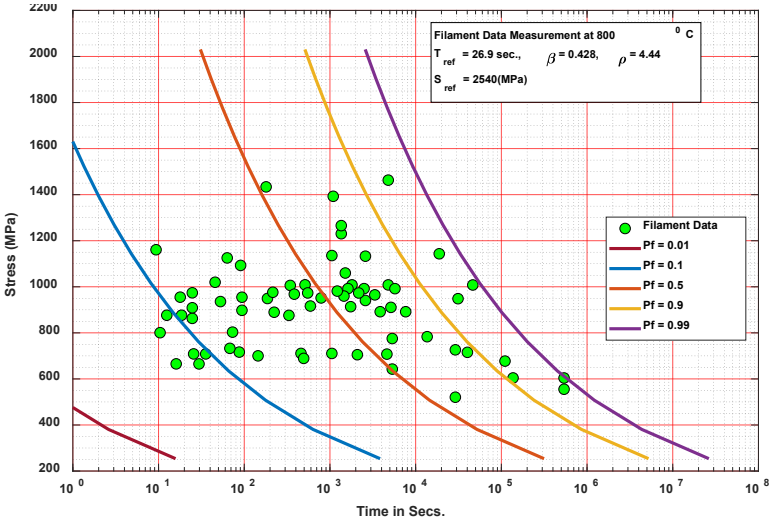

Figure 5.—Simulation of stress-rupture of single filaments of Hi-Nicalon at intermediate temperature. Green dots represent test data points from Reference 3, while curves represent simulations of various probabilities of failure (P_f).

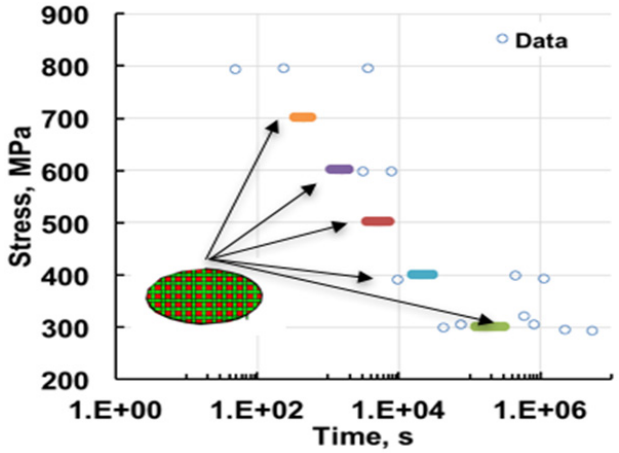

Figure 6.—Time to failure versus applied stress for Hi-Nicalon fiber tows at intermediate temperatures. Blue circles represent test data from Reference 3, while other color dots represent results from 100 fiber tow simulations.

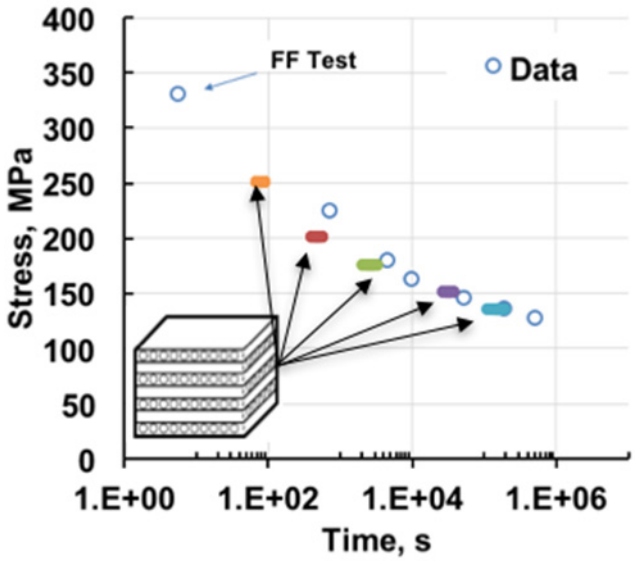

Figure 7.—Stress versus time-to-failure of Hi-Nicalon [0/90] SiC/SiC composites. Blue dots represent measured data, while other color dots represent results from 100 simulations each at various stress levels.

Stress versus time-to-failure of 2-D five-harness woven SiC/SiC composites reinforced by Hi-Nicalon fibers was also predicted at intermediate temperatures again using the calibrated parameters for single fibers. The [0/90] five-harness woven composite is approximated by a $[0/90]_s$ laminated composite in MAC/GMC computer code. 100 simulations were run for each stress level. Results are shown in Figure 7. The predictions are in generally good agreement with the measured data. Again, the observed scatter (from 100 simulations) is much less than what was observed in the single filament data. Simulation results indicate that as one moves up the length (volume) scale, the scatter that is observed in the results reduces.

The model used in the analyses above is based on the premise that the fibers have flaws of different initial sizes that grow with time in an oxidizing environment. In other words, initial fiber strength has significant variability, and that's what causes the variability in time-to-failure under constant applied stress. Variability in fiber strength can be due to initial voids, pores or cracks in addition to any material nonuniformity that the fiber material may have. It is also known that the fiber diameter is not constant. It also has a significant variation. Nominal value of the fiber diameter is mentioned as 14 μm based on average density and mass of a given length of the fiber. Fiber diameter is known to vary anywhere from 7 to 21 μm (Ref. 20). Figure 8 shows mean diameter versus standard deviation of 30 filament measurements. A total of 3000 measurements were made (Ref. 20). Additionally, fiber strength is a calculated value and not directly measured. It is computed as the applied load at failure divided by the cross-sectional area based on the nominal diameter. Fiber may not necessarily fail at the location of minimum diameter but it may fail at a location where the flaw size is largest or a combination thereof. Since the fiber location at failure is not precisely known, the fiber diameter is also not known at the location of fiber failure. In case of a composite, fibers bridge the matrix cracks/flaws. Because of that, there are stress risers in fiber in proximity to matrix cracks or flaws. It also makes it more likely for the fiber to fail at this location which again may not be the location of minimum fiber diameter or the location of largest flaw in the fiber. Causes of fiber variation are shown schematically in Figure 9.

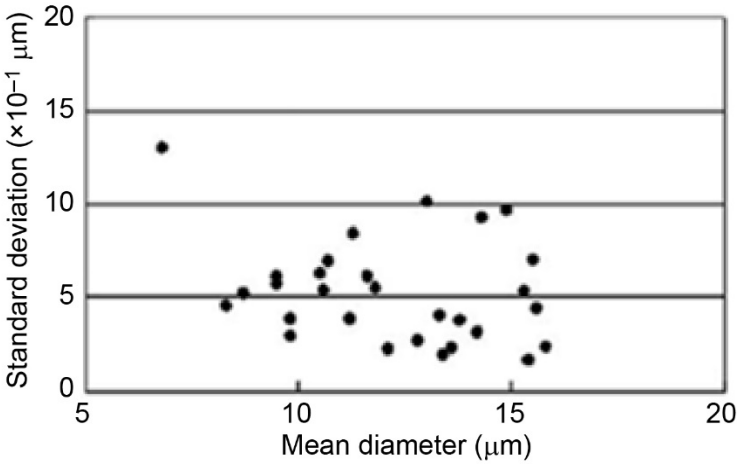

Figure 8.—Mean diameters versus standard deviation for Hi-Nicalon Type S monofilaments, Measurements of 30 Monofilaments from Reference 20.

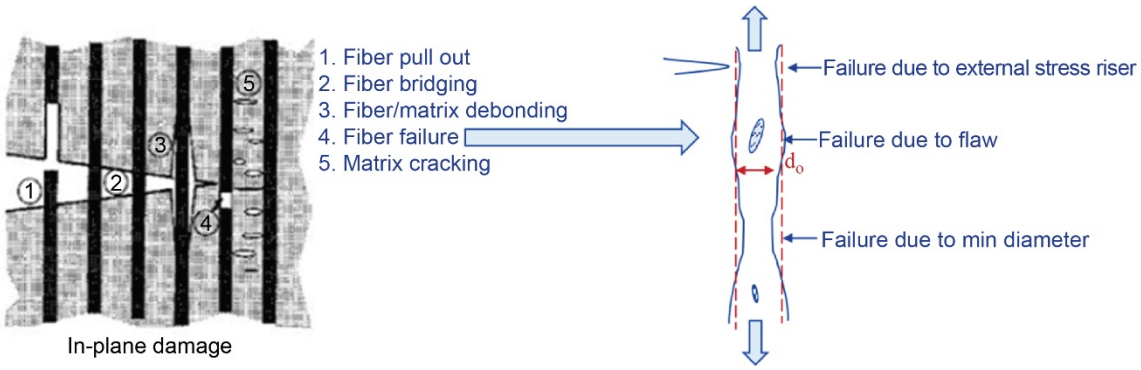

Figure 9.—Causes of variation in fiber strength.

There is a significant scatter in the time-to-failure versus applied stress in case of single filaments as shown in Figure 4. Since the actual diameter of the filament at failure location is not known, the applied stress is therefore not precisely known either. During testing, a constant load is applied so the actual stress along the fiber length varies significantly as the fiber diameter varies. It is possible if the fiber diameter could be measured in the gage length and if possibly the failure location could also be pinpointed precisely, then one would have a much better idea of applied stress at the failure location and the scatter shown in Figure 4 could be significantly minimized. Even though, the direct measurement of fiber diameter through laser interferometry requires expensive setup, finding the exact location of fiber failure has proved to be extremely difficult because of the very brittle nature of silicon carbide fiber (Ref. 20). Therefore, even with the direct measurements of fiber diameter in the gage length, unless the exact location of the fiber failure is also known, one cannot separate the effects of above mentioned causes on the variation of fiber strength. Even if all this could be accomplished somehow, results clearly indicate that as we move up the length (volume) scale from single fibers to tows to a multitow composite, the scatter in time-to-failure at an applied stress decreases. Thus, even if we could get the data at the single filament level “more accurately” having less scatter, it may not make much of a difference at higher scales particularly at the laminate or possibly at the sub-component or coupon (not shown here) level. It should also be mentioned that there are variations in volume fractions, ply angles, ply thicknesses etc. which prevent us from being able to compute the applied stresses in a laminate very accurately. Thus obtaining a very high fidelity data at a lower scale may not make much sense or difference in the results at higher length scales.

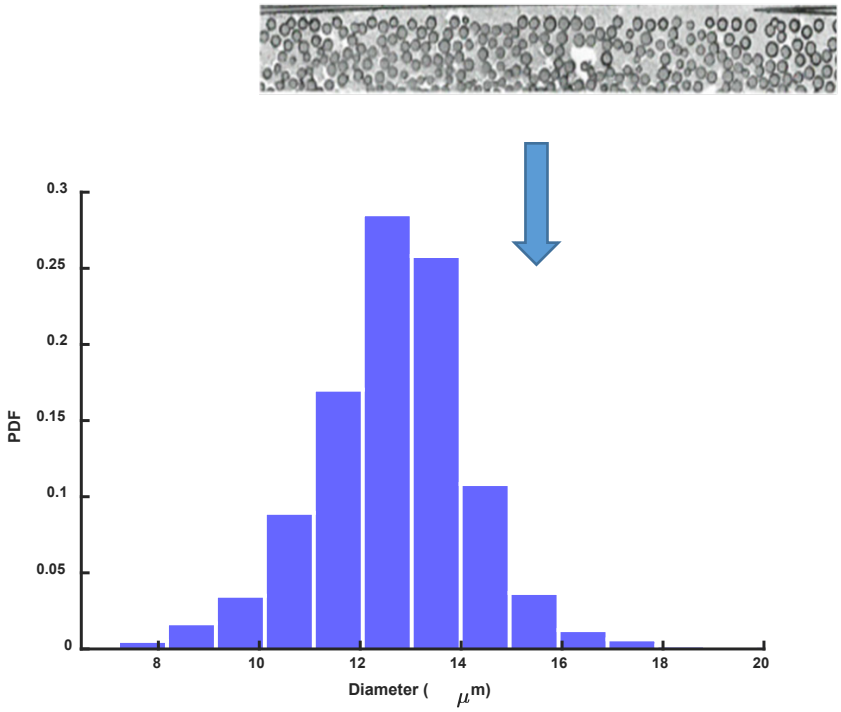

Figure 10.—Image analysis of a micrograph to obtain a histogram of fiber diameters.

However, if fiber diameter variation is desired, it may be much more cost effective to perform image analysis on high-resolution micrographs as compared to direct measurement using some sort of a laser technique. These type of analyses can provide this information quite efficiently. We have developed a MATLAB GUI-based image analysis tool and a sample result in shown in Figure 10.

Conclusions

Silicon carbide fibers, fiber tows and SiC/SiC composites display strength degradation or delayed failure under constant applied load at intermediate temperatures. It is assumed in the present work that time-dependent strength degradation phenomenon in Hi-Nicalon fibers is inherently due to slow growth of flaws in the fibers. It is believed that this mechanism is enabled by the presence of an oxidizing environment. No other mechanism such as the oxidation of the fiber coating or the oxidation of the silicon carbide fiber itself was included in the analyses shown here. An algorithm based on progressive failure and the "fiber classic model" was developed and implemented as a user-function in NASA's micromechanics-based MAC/GMC computer code. The new capability in the MAC/GMC computer code was exercised and the model parameters were calibrated from individual filament data and the maximum likelihood estimation (MLE) technique. Using these calibrated parameters, the prediction of stress versus time-to-failure of fiber tow was made and compared with available data. Predictions show that as the applied stress is increased the time-to-failure decreases and the observed scatter is much less than what was observed in single filament data/predictions. The trend in the measured data is not so clear for the dry tows. The predictions were also made for a [0/90] SiC/SiC composite time-to-failure versus applied composite stress. Those predictions compared well with the measured data. Same trend was noticed again that as we increase the applied composite stress, the time-to-failure decreases. As we move up from single filament to tows to multiply laminates, the scatter in the time-to-failure decreases. Results indicate that the strength degradation of the silicon carbide fibers can be entirely attributed to the slow growth of flaws in the fibers.

References

1. Zok, F.W., "Ceramic-Matrix Composites Enable Revolutionary Gains in Turbine Engine Efficiency," American Ceramic Society Bulletin, 95[5] 22–28 (2016).
2. Morscher, G.N. and Cawley, J.D., "Intermediate Temperature Strength Degradation in SiC/SiC Composites," Journal of European Ceramic Society, 22(2002) pp. 2777–2787.
3. Gauthier, W. and Lamon, J., "Delayed Failure of Hi-Nicalon and Hi-Nicalon S Multifilament Tows and Single Filaments at Intermediate Temperatures (500° – 800 °C)", J. Am. Ceram. Soc. 92[3] 702–709 (2009).
4. Sullivan, R.M., "Time-Dependent Stress-Rupture Strength of Hi-Nicalon Fiber-Reinforced Silicon Carbide Composites at Intermediate Temperatures," Journal of European Ceramic Society, 36(2016) pp. 1885–1892.
5. Parthasarthy, T.A.; Cox, B.; Sudre, O.; Przybyla, C.; and Cinibulk, M.K., "Modeling Environmentally Induced Property Degradation of SiC/BN/SiC Ceramic Matrix Composites," J. Am. Ceram. Soc. 101[3] 973–997 (2017).
6. Yun, H.M. and DiCarlo, J.A., Ceram. Eng. Sci. Proc., 4, 61–7 (1996).
7. Morscher, G.; Hurst, J., and Brewer, D., "Intermediate-Temperature Stress Rupture of a Woven Hi-Nicalon, BN-Interphase, SiC-Matrix Composite in Air," J. Am. Ceram. Soc. 83[6] 1441–1449 (2000).
8. Heredia, F.E.; McNulty, J.C.; Zok F.W. and Evans A.G., "Oxidation Embrittlement Probe for Ceramic Matrix Composites," J. Am. Ceram. Soc. 78 [8] 2097–2100 (1995).
9. Xu, W.; Zok, F. and McMeeking, R., "Model of Oxidation-Induced Fiber Fracture in SiC/SiC Composites," J. Am. Ceram. Soc. 1–8 (2014).
10. Lara-Curzio, E., "Stress-Rupture of Nicalon/SiC Continuous FiberCeramic Composites in Ait at 950 C," J Am. Ceram. Soc. 80[12] 3268–3272 (1997).
11. Forio, P.; Lavaire, F., and Lamon, J., "Delayed Failure at Intermediate Temperatures (600-700 C) in Air in Silicon Carbide Multifilament Tows," J. Am. Ceram. Soc. 87[5] 888–893 (2004).
12. Gauthier, W.; Pailler, F; Lamon, J., and Pailler, R., "Oxidation of Silicon Carbide Fibers During Static Fatigue in Air at Intermediate Temperatures," J. Am. Ceram. Soc. 92[9] 2067–2073 (2009).
13. Murthy, P.L.N; Thesken, J.C.; Phoenix, S.L., and Grimes-Ledesma, L., "Stress Rupture Life Reliability Measures for Composite Overwrapped Pressure Vessels," NASA/TM—2007-214848, June 2007.
14. MAC/GMC 4.0 User's Manual—Example Problem Manual, NASA/TM—2002-212077, December 2002.
15. Paley M. and Aboudi J., "Micromechanical Analysis of Composites by the Generalized Cells Model," Mech. Mater 1992; 14: 127–139.
16. Aboudi J., Arnold S.M. and Bednarcyk B.A., "Micromechanics of Composite Materials: A Generalized Multiscale Analysis Approach," Waltham, MA, USA: Elsevier, Inc., 2013.
17. Davidge, R.W.; McLaren, J.R. and Tappin, G., "Strength-Probability-Time (SPT) Relationships in Ceramics," J. of Materials Science 8 1699–1705 (1973).
18. Coleman, B.D., "Statistics and Time Dependence of Mechanical Breakdown in Fibers," Journal of Applied Physics, 29 (1958): 968.
19. Ang, A. and Tang, W., "Probability Concepts in Engineering," 2nd edition, John Wiley & Sons, Inc. 2007.
20. Morimoto, T. and Ogasawara, T., "Potential Strength of Nicalon, Hi-Nicalon and Hi-Nicalon Type S Monofilaments of Variable Diameters," Composites, Part A: Applied Science and Manufacturing, 37, 405–412 (2006).